Gene Expression Changes in Areas of Focal Loss of Retinal Ganglion Cells in the Retina of DBA/2J Mice

Lampros Panagis,[1] *Xiujun Zhao,*[1] *Yongchao Ge,*[2] *Lizhen Ren,*[1] *Thomas W. Mittag,*[1,3] *and John Danias*[1,4]

Purpose. To determine whether differences in gene expression occur between areas of focal retinal ganglion cell (RGC) loss and of relative RGC preservation in the DBA/2 mouse retina and whether they can provide insight into the pathophysiology of glaucoma.

Methods. Areas of focal RGC loss (judged by lack of Fluorogold labeling; Fluorochrome, Denver, CO), adjacent areas with relative RGC preservation in DBA/2 retina, and Fluorogold-labeled retina from DBA/2^{-pe} (pearl) mice were dissected and used for microarray analysis. RT-PCR and immunoblot analysis were used to confirm differential gene expression. Bioinformatic analysis was used to identify gene networks affected in the glaucomatous retina.

Results. Microarray analysis identified 372 and 115 gene chip IDs as up- and downregulated, respectively, by 0.5-fold in areas of RGC loss. Differentially expressed genes included those coding for cytoskeletal proteins, enzymes, transport proteins, extracellular matrix (ECM) proteins, and immune response proteins. Several genes were confirmed by RT-PCR. For at least two genes, differential protein expression was verified. Bioinformatics analysis identified multiple affected functional gene networks. Pearl mice appeared to have significantly different gene expression, even when compared with relatively preserved areas of the DBA/2 retina.

Conclusions. Regional gene expression changes occur in areas of focal RGC loss in the DBA/2 retina. The genes involved code for proteins with diverse cellular functions. Further investigation is needed to determine the cellular localization of the expression of these genes during the development of spontaneous glaucoma in the DBA/2 mouse and to determine whether some of these gene expression changes are causative or protective of RGC loss. (*Invest Ophthalmol Vis Sci.* 2010;51: 2024–2034) DOI:10.1167/iovs.09-3560

Murine models of glaucoma have been the subject of extensive investigation in the past few years in an effort to understand the pathophysiologic mechanisms that lead to the human disease.[1–3] One of the underlying assumptions is that by studying highly inbred mouse strains, one can decrease the biological variability that undoubtedly affects a complex disease process such as glaucoma.

The DBA/2 mouse strain has emerged as one of the most representative animal models of human glaucoma.[1,4] Even though this mouse strain exhibits anterior segment abnormalities that include iris atrophy, pigment dispersion, and peripheral anterior synechiae, which are different from what happens in the human open-angle glaucomas, it is the development of elevated intraocular pressure (IOP; starting at ~6 months of age)[5,6] and progressive optic neuropathy that has justified the use of this mouse as a model for the study of the posterior segment processes that operate in human glaucoma.

The pathologic changes in the retina and optic nerve are progressive and affect most of the female mice starting at about 9 months of age.[1] Histologic study of the eyes at later ages has shown a thinning of the nerve fiber layer, retinal ganglion cell (RGC) loss, and optic nerve atrophy.[1] However, this degenerative process is not uniform.[6,7] RGCs in the DBA/2 mouse retina die in patches in a manner reminiscent of focal RGC loss in the human disease.[6,8] We reasoned that this preferential loss of some RGCs early in the development of murine glaucoma is paralleled by changes in gene expression within the retina. In the present study, we used microarray analysis to determine differences in gene expression between areas of focal RGC loss and areas of relative RGC preservation in the retina of the DBA/2 mice, in an effort to better understand the pathophysiology of murine glaucoma.

Methods

All animals were handled in accordance with the ARVO Statement for the Use of Animals in Ophthalmic and Vision Research. A group of 11- to 15-month-old DBA/2 female mice ($n = 10$) from the colony that we maintain at the Mount Sinai School of Medicine was used in the experiments. Pearl mice (DBA/$2J^{-pe}$), were also obtained from Jackson Laboratories (Bar Harbor, ME), and a colony was established and kept at the Mount Sinai School of Medicine. These animals (female of same age, $n = 4$) served as the nonpathologic control, as they are on a DBA/2 background but do not develop significant retinal disease or RGC loss, at least until the 15th month of age. The animals were housed in covered cages, fed with a standard rodent diet ad libitum, and kept in a constant 12-hour light/12-hour dark cycle.

The mice were anesthetized with a mixture of xylazine, acepromazine, and ketamine. Their skulls were exposed, and holes approximately 2 mm in diameter were drilled bilaterally to expose the occipital cortex. Under constant direct observation, the occipital cortex overlying the superior colliculus (SC) was gently aspirated, and the SC was exposed. A piece of gel foam (Pharmacia & Upjohn, Kalamazoo, MI) soaked in 5% aqueous Fluorogold (Fluorochrome, Denver, CO) was applied to each SC. The gel foam was covered with antibiotic ointment, and the overlying skin was sutured. The animals were killed 4 days later, the eyes were enucleated, and the retinas were removed and flat mounted in preservative (RNAlater; Ambion, Inc., Austin, TX). Flatmounts were immediately examined for areas of focal RGC loss

From the Departments of [1]Ophthalmology, [2]Neurology, [3]Pharmacology, and [4]Neuroscience, Mount Sinai School of Medicine, New York, New York.

Supported by National Eye Institute Grants EY15224, EY16050, and EY0186 and Research to Prevent Blindness.

Submitted for publication February 12, 2009; revised May 31 and July 13, 2009; accepted July 14, 2009.

Disclosure: **L. Panagis**, None; **X. Zhao**, None; **Y. Ge**, None; **L. Ren**, None; **T.W. Mittag**, None; **J. Danias**, None

Corresponding author: Lampros Panagis, Department of Ophthalmology, 1183, Mount Sinai School of Medicine, 1 Gustave L. Levy Place, New York, NY 10029; lampros.panagis@downstate.edu.

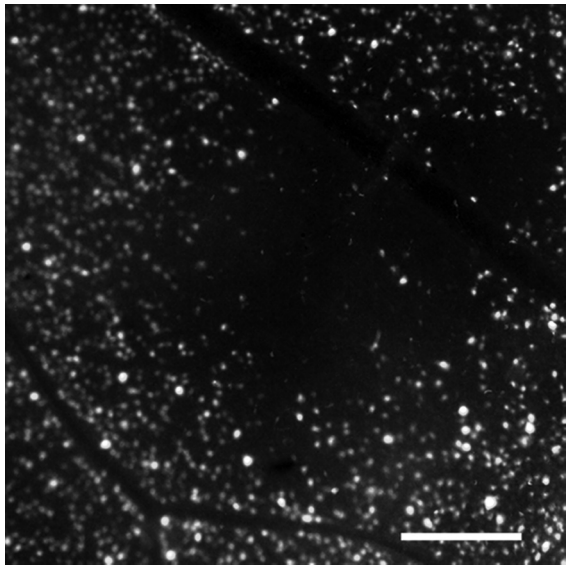

FIGURE 1. Typical area of early, focal RGC loss in DBA/2 mouse retina. Scale bar, 100 μm.

(Fig. 1). In retinas in which such areas were detected, areas of focal loss and adjacent areas with relative RGC preservation were dissected and stored (RNAlater; Ambion). Both DBA/2 and DBA/2J^{-pe} mice were labeled with Fluorogold 4 days before death.

Microarray Gene Expression Profiling

Ten DBA/2 mice were used in the project. RNA was extracted from retinal tissue (TRIzol method; Qiagen, Valencia, CA) after the tissue was washed carefully with DEPC-treated water to remove traces of preservative (RNAlater; Ambion). Briefly, the tissue was homogenized in the extraction agent, and chloroform was added to separate the proteins from the RNA. After centrifugation, the RNA-containing supernatant was aspirated, and the organic phase was used for protein extraction. The RNA was washed with isopropanol, precipitated in 70% ethanol, and column purified (RNAeasy mini kit; Qiagen), per the manufacturer's instructions, and subjected to microarray analysis. Proteins were extracted from the organic phase by dialyzing in cellulose dialysis tubing against three changes of 0.1% SDS at 4°C for 48 hours. Protease inhibitors were added, and the samples were stored at −80°C until subjected to immunoblot analysis. RNA quality control testing was performed (Bioanalyzer; Agilent, Palo Alto, CA) based on the UCLA data quality guide (http://core.genetics.ucla.edu/public/EDCGuidelines). Linear amplification, cRNA synthesis and hybridization to mouse oligonucleotide arrays (GeneChip Mouse Genome 430_2.0; Affymetrix, Santa Clara, CA) was performed at the Mount Sinai core microarray facility. Signal intensities for ~45,000 probe sets (each probe set consisting of 11 perfect matches and 11 mismatches) were obtained from each array. Data quality was verified by inspection of various plots of the probe signal intensities such as histograms, box plots, and RNA degradation plots as well as different quality metrics, such as the percentage of probe sets that are called "present" by the MAS 5.0 algorithm,[9] the average background, the scale factor and the GAPDH and β-actin 3′:5′ ratios. Arrays failing quality control were replaced with additional arrays. Four paired sets of retinal samples from individual eyes with focal damage were used for statistical analysis.

Probe intensities of the whole dataset were processed using the Gene Chip Robust Multi-array (gcrma)[10] package in Bioconductor.[11] The gcrma package adjusts for background intensities in Affymetrix array data, which include optical noise and nonspecific binding and converts background-adjusted probe intensities to expression measures after normalization. The summarized data are thus normalized signal intensities that are logarithm base 2 (log2) transformed. These summarized data were then subjected to statistical analysis.

Real-Time PCR Gene Expression Quantification

Real-time PCR (RT-PCR) was performed to confirm several of the genes identified to be differentially expressed in the microarray analysis. RNA from paired samples from areas of focal loss and adjacent areas with relative RGC preservation were reverse transcribed with random primers to cDNA with a kit (Quantitect; Qiagen), per the manufacturer's instructions. cDNA was prepared for RT- PCR with a SYBR Green RT-PCR Kit (QuantiTect; Qiagen) and specific primer sets (SuperArray Biosciences, Frederick, MD; Table 1). The samples were analyzed at the Mount Sinai RT-PCR Core Facility.

TABLE 1. Primer Sets Used for RT-PCR Expression Quantification Experiments

Superarray Primer*	RefSeq Accession†	Symbol	Gene Name (Affymetrix‡)
PPM34399E	NM_007585	*Anxa2*	Annexin A2
PPM04133A	NM_013477	*Atp6v0d1*	ATPase, H+ transporting, lysosomal V0 subunit D1
PPM05302A	NM_007902	*Edn2*	Endothelin 2
PPM35275A	NM_001081081	*Gls*	Glutaminase
PPM04054E	NM_010610	*Kcnma1*	Potassium large conductance calcium-activated channel, subfamily M, alpha member 1
PPM03405E	NM_008562	*Mcl1*	Myeloid cell leukemia sequence 1
PPM24537A	NM_008638	*Mthfd2*	Methylenetetrahydrofolate dehydrogenase (NAD+ dependent), methenyltetrahydrofolate cyclohydrolase
PPM24964E	NM_010863	*Myolb*	Myosin 1B
PPM33303A	NM_177215	*Ocrl*	Oculocerebrorenal syndrome of Lowe
PPH08362A	NM_024586	*Osbpl9*	Oxysterol binding protein-like 9
PPM30599A	XM_001477215	*Sbf2*	SET binding factor 2
PPM35412A	NM_080853	*Slc17a6*	Solute carrier family 17 (sodium-dependent inorganic phosphate cotransporter), member 6
PPM27769A	NM_009229	*Sntb2*	Basic 2 Syntrophin
PPM41859E	NM_178871	*Tbrg3*	Transforming growth factor beta regulated gene 3
PPM34132E	NM_153162	*Txnrd3*	Thioredoxin reductase 3
PPM37650A	NM_145514	*Wdr26*	WD repeat domain 26

* SuperArray Biosciences, Frederick, MD.

† RefSeq is provided in the public domain by the National Center for Biotechnology Information (Bethesda MD) and is available at www.ncbi.nlm.nih.gov/locuslink/refseq/.

‡ Santa Clara, CA.

Immunoblot Analysis

Protein samples were diluted in loading buffer, separated in a 4% to 20% SDS-PAGE gel (Bio-Rad, Hercules, CA), and transferred to PVDF membranes. The membranes were then blocked (Superblock; Thermo Fisher Scientific, Rockford, IL) and incubated with a goat polyclonal anti-Osbpl-9 antibody (Abcam, Cambridge, MA) (1:1000, overnight at 4°C) or a goat polyclonal anti-β2-syntrophin antibody (1:1000, overnight at 4°C; Santa Cruz Biotechnology, Santa Cruz, CA), followed by incubation with an HRP-conjugated anti-goat IgG antibody for 2 hours at room temperature. A rabbit anti-β-actin-specific antibody (1:5000, overnight at 4°C; Abcam) was used to verify that equal amounts of protein had been loaded in each lane. Antibody binding was visualized with chemiluminescence (ECL; Pierce, Rockford IL) on an image station (model 440CF; Kodak, Boston, MA) and quantified with ImageJ image-analysis software (developed by Wayne Rasband, National Institutes of Health, Bethesda, MD; available at http://rsb.info.nih.gov/ij/index.html) after normalization for actin concentration.

Statistical and Bioinformatics Analysis

Principal component analysis (PCA) was performed to determine the differences in global gene expression between damaged retinal areas in DBA/2 mice, spared retinal areas in the same animals, and retinas of pearl mice. PCA transforms the microarray samples with thousands of gene expression measurements into principal components (PCs) that are not correlated with each other and that account for decreasing proportions of the total variances. Each PC is defined as a particular linear combination of the original genes. In plots with two PCs, each sample is represented by the projection of the original sample onto these two PCs.

In addition, retinal samples from DBA/2 retinas were compared as pairs. For each gene, the comparison between areas of retina with severe RGC loss and those with relative preservation was based on a moderated *t*-statistic, defined to be $(\bar{x} - \bar{y}) / s + s_0)$, where $\bar{x}$, $\bar{y}$ are the average log2 signal intensities from the gcrma package for the two groups, respectively, and s is the standard error of the $\bar{x} - \bar{y}$, equal to $\sqrt{s_x^2/n_x + s_y^2/n_y}$. s_0 takes the 10th percentile of s among 45,000 probe sets, which is used to make sure the two-sample *t*-statistic does not become extremely large, just because of an extremely small s. Significant genes were selected by the following criteria: a moderated *t*-statistic no less than 3 in absolute value, a maximum signal intensity no less than 5, and a log2-fold change ($\bar{x} - \bar{y}$ no less than 0.5 in absolute value.

Chip IDs (Affymetrix) that were identified to be differentially expressed were manually curated to determine whether they correspond to specific genes or represent only ESTs that cannot be assigned to any specific genes.

Table 2. Upregulated Genes in Areas with Significant RGC Loss in the DBA/2 Retina

Gene Symbol	Ref Seq Accession*	Mod.t	Log2.fd	Gene Name (Affymetrix*)
Cald1	NM_145575	10.86	0.87	Caldesmon 1
9430051O21Rik	—	9.15	1.19	RIKEN cDNA 9430051O21 gene
2900046L07Rik	—	8.61	0.75	RIKEN cDNA 2900046L07 gene
Arib1	NM_019927	8.41	0.83	Ariadne ubiquitin-conjugating enzyme E2 binding protein homolog 1 (Drosophila), mRNA (cDNA Clone MGC: 47121 IMAGE:4035861)
Abce1	NM_015751	8.41	0.64	ATP-binding cassette, sub-family E (OABP), Member 1
Nisch	NM_022656	7.93	0.53	Nischarin
Polb	NM_011130	7.69	0.51	Polymerase (DNA directed), beta
Farsla	NM_025648	7.69	0.68	Phenylalanine-tRNA synthetase-like, alpha subunit
BC021395	NM_144861	7.57	0.57	CDNA sequence BC021395 (BC021395), mRNA
Ocr1	NM_177215	7.56	0.69	Oculocerebrorenal syndrome of Lowe
Gpsn2	NM_134118	7.5	0.5	ES cells cDNA, RIKEN full-length enriched library, clone: 2410016D23 product:SC2 homolog [Rattus sp], full insert sequence
Stk22s1	NM_011651	7.27	0.81	Serine/threonine kinase 22 substrate 1
Rbm18	NM_026434	7.23	0.61	RNA binding motif protein 18
5730410E15Rik	NM_178765	7.19	0.62	M-Golsyn mRNA for Golgi-localized syntaphilin-related protein A
A230071A22Rik	-	7.16	0.79	RIKEN cDNA A230071A22 gene
AA960558	NM_133942	7.01	0.61	Pleckstrin homology domain containing, family A (phosphoinositide binding specific) member 1 (Plekhal), mRNA
Pbx1	NM_183355	6.77	0.89	Pre B-cell leukemia transcription factor 1, mRNA (cDNA clone MGC:7546 IMAGE:3492658)
Rpgrip1	NM_023879	6.57	0.55	Retinitis pigmentosa GTPase regulator interacting protein 1
Tbc1d23	NM_026254	6.51	0.55	TBC1 domain family, member 23
Tbc1d5	NM_028162	6.39	0.87	TBC1 domain family, member 5
9630002A11Rik	-	6.37	0.57	RIKEN cDNA 9630002A11 gene
BC004004	NM_030561	6.36	1.06	cDNA sequence BC004004
Trim24	NM_145076	6.36	0.67	Tripartite motif protein 24
Psmd14	NM_021526	6.29	0.51	Proteasome (prosome, macropain) 26S subunit, non-ATPase, 14, mRNA (cDNA clone MGC:5840 IMAGE: 3599671)
Igf2bp2	NM_183029	6.2	2.67	Insulin-like growth factor 2 mRNA binding protein 2
Rab37	NM_021411	6.16	0.97	RAB37, member of RAS oncogene family
Foxn2	NM_180974	6.09	0.58	Forkhead box N2
Wwp1	NM_177327	6.03	0.63	WW domain containing E3 ubiquitin protein ligase 1
Ctnna1	NM_009818	5.81	0.57	Cadherin associated protein), alpha 1
Polr3f	NM_029763	5.8	0.65	Polymerase (RNA) III (DNA directed) polypeptide F

* See the footnote to Table 1.

TABLE 3. Downregulated Genes in Areas with Significant RGC Loss in the DBA/2 Retina

Gene Symbol	RefSeq Accession*	Mod.t	Log2.fd	Gene Name (Affymetrix*)
Cul5	NM_027807	−14.71	−1.21	Cullin 5
Lxn	NM_016753	−11.36	−0.66	Latexin
Opa1	NM_133752	−10.7	−0.62	Optic atrophy 1 homolog (human)
Mthfd2	NM_008638	−10.6	−1.14	Methylenetetrahydrofolate dehydrogenase (NAD+ dependent), methenyltetrahydrofolate cyclohydrolase
Tatdn1	NM_175151	−9.85	−0.54	TatD DNase domain containing 1
Sh2bp1	NM_009431	−8.61	−0.53	SH2 domain binding protein 1 (tetratricopeptide repeat containing)
Fzd1		−8.21	−0.56	Frizzled homolog 1 (Drosophila)
Anxa2	NM_007585	−8.18	−0.83	Annexin A2
Fstl5	NM_021457	−7.26	−0.54	Follistatin-like 5
Fyttd1	NM_007585	−7	−0.54	Forty-two-three domain containing 1
Ppp2r5e	NM_012024	−7	−0.54	Protein phosphatase 2, regulatory subunit B (B56), epsilon isoform
Zfp318	NM_021346	−6.79	−0.6	Zinc finger protein 318
Spin2	NM_001005370	−6.48	−0.71	Spindlin-like
Rgs10	NM_026418	−6.21	−0.56	Regulator of G-protein signalling 10
Egln1	NM_053207	−6.17	−0.54	EGL nine homolog 1 (C. elegans)
Zfp292	XM_620009	−6.02	−1.04	Zinc finger protein 292
Hdlbp	NM_133808	−5.96	−0.89	High density lipoprotein (HDL) binding protein
Acbd3	NM_133225	−5.9	−0.72	Acyl-Coenzyme A binding domain containing 3
Spock1	NM_009262	−5.58	−0.85	Sparc/osteonectin, cwcv and kazal-like domains proteoglycan 1
Emb	NM_010330	−5.53	−0.63	Embigin
Tpmt	NM_016785	−5.5	−1.02	Thiopurine methyltransferase
Rgs9	NM_011268	−5.46	−0.57	Regulator of G-protein signaling 9
Satb1	NM_009122	−4.98	−0.54	Special AT-rich sequence binding protein 1, mRNA (cDNA clone MGC:18461 IMAGE:4164993)
Usp45	NM_152825	−4.9	−0.91	Ubiquitin-specific peptidase 45
Ociad2	NM_026950	−4.9	−0.52	OCIA domain containing 2
Kif1b	NM_008441	−4.84	−0.78	Kinesin family member 1 B
Pon3	NM_173006	−4.8	−0.5	Paraoxonase 3
8430439J12Rik	XM_287445	−4.76	−0.67	RIKEN cDNA 8430439J12 gene
C230085N15Rik	—	−4.74	−0.53	RIKEN cDNA C230085N15 gene
Epb4.112	NM_013511	−4.72	−0.5	Erythrocyte protein band 4.1-like 2

* See the footnote to Table 1.

Genes thus selected were subjected to bioinformatics analysis by pathway-analysis software (Ingenuity Systems; Redwood City, CA and DAVID bioinformatics resources; http://david.abcc.ncifcrf.gov/ provided in the public domain by the National Cancer Institute, Frederick, MD) to determine functional gene networks and canonical groups whose expression is differentially affected between areas of focal RGC loss and those with relative preservation.

RESULTS

Gene expression in the healthy retina of the pearl mice was significantly different from that in undamaged (spared) areas of the DBA/2 mice, as judged from PCA of the signal intensities of all genes included in the microarray (Affymetrix), suggesting that even in areas without apparent RGC loss in DBA/2 mice, pathologic processes that lead to such a loss are operational. Although retinal samples from DBA/2 mice were paired (originating from the same retinas), samples from pearl mice were not. Consequently, when the three groups were compared by ANOVA (using the same criteria for significance described earlier) the number of genes with differential expression between pearl and DBA/2 retinal areas (either damaged or spared) was rather large (>5000 differentially expressed genes for both comparisons).

By comparing four sets of paired samples of damaged and relatively spared areas in the retinas of DBA/2 mice, we identified 487 IDs with different levels of expression of at least 0.5 log2-fold change between damaged and preserved areas of DBA/2 retinas. The expression of 372 IDs was upregulated, whereas that of 115 was downregulated in areas of RGC loss. Of these, 357 were mapped to mRNA messages of genes (rather than ESTs or genomic sequences). The first 30 (most significant) of the up- and downregulated genes and their modified *t*-statistic (mod.t) and log2-fold (log2.fd) changes are shown in Tables 2 and 3, respectively. (The full Affymetrix ID list can be viewed as Supplementary Material at http://www.iovs.org/cgi/content/full/51/4/2024/DC1.)

When expression levels of these genes were compared with those in pearl retinas, 219 of them were expressed at either similar levels between spared areas and pearl retinas or showed a progressive change from pearl, to spared, to damaged areas. Surprisingly, for 138 genes, expression in pearl retinas was closer to the level in damaged DBA/2 retinal areas (rather than in spared areas). The first 30 (most significant) of the up- and downregulated genes in undamaged and damaged DBA/2 retinal areas compared with pearl retinas and their mod.t and log2-fd changes are shown in Tables 4 and 5, respectively. (The full Affymetrix ID list can be viewed as Supplementary Material at http://www.iovs.org/cgi/content/full/51/4/2024/DC1.)

Further bioinformatic pathway analysis (Ingenuity) revealed that genes with differential expression belonged to at least 22 functional networks. The most heavily populated network included 26 genes (of 35 genes included in the network) and is related to cellular assembly and organization, growth, and proliferation and visual system development and function (Fig. 2). Since these networks are somewhat arbitrary (based on the known relationships of molecules) the same molecules can participate in two or more networks. Thirteen of the networks identified overlapped by one or more molecules, linking at least 438 genes, of which 206 (47%) appeared to change expression. When the genes were organized into canonical pathways, phototransduction, tight-junction signaling, EGF signaling, and inositol diphosphate metabolism were the most affected.

TABLE 4. Genes Exhibiting Expression Changes in Areas with RGC Preservation in the DBA/2 Retina Compared with the Pearl Retina

Gene Symbol	RefSeq Accession*	Mod.t	Log2.fd	Gene Name (Affymetrix*)
Upregulated genes				
Scnm1	NM_027013	16.85	3.59	Sodium channel modifier 1
Top2b	NM_009409	15.47	2.93	Topoisomerase (DNA) II beta
Lztfl1	NM_033322	15.26	2.38	Leucine zipper transcription factor-like 1
Mest	NM_008590	13.93	2.05	Mesoderm specific transcript
Irb	NM_001113356, NM_023143, XM_001002804, XM_001480171	13.14	1.04	Complement component C1rb
Impg1	NM_022016	12.11	0.89	Interphotoreceptor matrix proteoglycan 1
Ermap	NM_013848	12.01	2.36	Erythroblast membrane-associated protein
C3	NM_009778	11.68	3.70	Complement component 3
Tnpo1	NM_001048267, NM_178716	11.25	1.46	Transportin 1
G6pd2	NM_008062, NM_019468	11.21	3.45	Glucose-6-phosphate dehydrogenase 2
Als2cr4	NM_001033449, NM_001037812	11.09	1.07	Amyotrophic lateral sclerosis 2 (juvenile) chromosome region, candidate 4
Zfp445	NM_173364	11.06	2.13	Zinc finger protein 445
Sema3c	NM_013657	10.49	1.71	Sema domain, immunoglobulin domain (Ig), short basic domain, secreted, (semaphorin) 3C
Ncam1	NM_001081445, NM_001113204, NM_010875	10.16	1.68	Neural cell adhesion molecule 1
Mrc1	NM_008625	10.14	1.27	Mannose receptor, C type 1
Downregulated genes				
BC023969	—	−27.52	−3.90	cDNA sequence BC023969
Al506816	XM_001000526	−21.37	−4.61	Expressed sequence Al506816
Slc6a1	NM_178703	−20.59	−3.96	Solute carrier family 6 (neurotransmitter transporter, GABA), member 1
Lrrtm2	NM_178005	−20.30	−3.12	Leucine rich repeat transmembrane neuronal 2
Sesn3	NM_030261	−20.14	−2.18	Sestrin 3
Pum2	NM_030261	−17.51	−3.05	Pumilio 2 (*Drosophila*)
Cntn1	NM_007727	−16.05	−2.26	Contactin 1
Hdac2	NM_008229	−16.01	−2.39	Histone deacetylase 2
Timeless	NM_001136082, NM_011589	−15.08	−2.08	Timeless homolog (*Drosophila*)
Prkaa2	NM_178143	−14.79	−1.38	Protein kinase, AMP-activated, alpha 2 catalytic subunit
Rc3h2	NM_001100591, XM_130233, XM_925271	−14.62	−2.55	Ring finger and CCCH-type zinc finger domains 2
Zfp644	NM_026856, XM_001475996, XM_001478595	−14.52	−1.67	Zinc finger protein 644
Rab14	NM_026697	−13.93	−2.78	RAB14, member RAS oncogene family
Tbce1	NM_173038	−13.91	−1.51	Tubulin folding cofactor E-like
9030612M13Rik	NM_172458	−13.68	−1.97	RIKEN cDNA 9030612M13 gene

* See the footnote to Table 1.

In addition, these genes could be grouped by DAVID analysis into 12 functional clusters with a maximum enrichment score of 6.56. Functional annotation clustering gave 124 clusters with a maximum enrichment score of 7.92.

To confirm microarray results, we identified 10 of the genes belonging to different gene networks and confirmed their expression differences by RT-PCR (Fig. 3).

To determine whether changes in gene expression translate into changes in protein expression, we selected one of the upregulated (*Osbpl-9*/ORP9) and one of the downregulated (*Sntb2* β2-syntrophin) genes and determined by immunoblot analysis whether there were differences in the amount of their respective proteins. Protein quantity was shown to increase and decrease respectively in areas of focal RGC loss, in accordance with gene expression changes observed using microarray and RT-PCR gene expression quantification (Fig. 4).

DISCUSSION

Retinal ganglion cell loss in DBA/2 mice has been shown to be variable.[6,7,12] Early damage, as in human glaucoma, is focal in nature, occurring in patches.[6,8,13] The progressive nature of optic neuropathy and concurrent RGC loss that these animals sustain means that, over time, these focal areas of damage will expand to cover most of the retina. However, early on it appears that there are differences between areas of retina with significant degeneration and those that are seemingly normal in the same eye. We used microarrays to study gene expression differences between these retinal areas.

Microarray technology offers the advantage that it looks at global gene expression.[14,15] However, because of the large number of genes analyzed, it also has some inherent limitations.[16,17] A portion of the genes identified are false positives, and some genes with truly changing expression fail to be

TABLE 5. Genes Exhibiting Expression Changes (Upregulation or Downregulation) in Areas with RGC Loss in the DBA/2 Retina Compared with Pearl Retina

Gene Symbol	RefSeq Accession*	Mod.t	Log2.fd	Gene Name (Affymetrix*)
Upregulated genes				
A330076H08Rik	—	7.80	5.11	RIKEN cDNA A330076H08 gene
C3	NM_009778	24.09	3.77	Complement component 3
Cnnm4	NM_033570	4.37	3.75	Cyclin M4
Scnm1	NM_027013	19.17	3.63	Sodium channel modifier 1
Edn2	NM_007902	6.37	3.45	Endothelin 2
Lcn2	NM_008491	11.55	3.16	Lipocalin 2
Ifitm1	NM_001112715, NM_026820	6.33	2.95	Interferon induced transmembrane protein 1
Cacna2d4	NM_001033382	4.95	2.93	Calcium channel, voltage-dependent, alpha 2/ delta subunit 4
4833420D23Rik	—	9.15	2.89	RIKEN cDNA 4833420D23 gene
Tspan7	NM_019634	3.95	2.79	Tetraspanin 7
G6pd2	NM_008062, NM_019468	6.65	2.75	Glucose-6-phosphate Dehydrogenase 2
Ifngr2	NM_008338	4.10	2.61	Interferon gamma receptor 2
Atp1b2	NM_013415	4.25	2.60	ATPase, Na+/K+ transporting, beta 2 polypeptide
Steap4	NM_054098	10.00	2.58	STEAP family member 4
Gpbp1	NM_001122963, NM_028487	5.26	2.56	GC-rich promoter binding protein 1
Downregulated genes				
Kndc1	NM_177261	−31.54	−2.96	Kinase non-catalytic C-lobe domain (KIND) containing 1
Pou4f2	NM_138944	−29.59	−6.13	POU domain, class 4, transcription factor 2
BC023969	—	−25.71	−3.80	cDNA sequence BC023969
Tusc5	NM_177709	−23.88	−4.58	Tumor suppressor candidate 5
Prkaa2	NM_178143	−21.91	−1.77	Protein kinase, AMP-activated, alpha 2 catalytic subunit
Pum2	NM_030723	−21.81	−3.26	Pumilio 2 (Drosophila)
AI506816	XM_001000526	−20.90	−4.65	Expressed sequence AI506816
Pou4f1	NM_011143	−20.38	−5.08	POU domain, class 4, transcription factor 1
Plaa	NM_172695	−20.28	−1.90	Phospholipase A2, activating protein
Sesn3	NM_030261	−20.07	−2.26	Sestrin 3
Lrrtm2	NM_178005	−19.95	−3.09	Leucine rich repeat transmembrane neuronal 2
Nefm	NM_008691	−19.81	−3.81	Neurofilament, medium polypeptide
Capn5	NM_007602	−16.77	−1.39	Calpain 5
Elavl2	NM_010486, NM_207685, NM_207686	−16.10	−2.84	ELAV (embryonic lethal, abnormal vision, Drosophila)-like 2
Bcl11b	NM_001079883, NM_021399	−16.08	−2.07	B-cell leukemia/lymphoma 11B

* See the footnote to Table 1.

identified. In addition genes with low-fold change are less likely to be detected than genes with dramatic changes in expression. Despite methodologic limitations, microarrays have been used in studying differential gene expression in relationship to glaucoma.[18–24] However, to date no one has systematically investigated gene expression differences in areas of the mouse retina that are damaged or spared, with respect to RGC loss. The advantage of using such an approach is that it significantly decreases biological variability as samples are paired, with each pair originating from one retina. In a disease process with such interanimal and intereye variability,[6,7] this approach provides a critical advantage in trying to narrow the number of potential genes involved.

To overcome some of the inherent limitations of microarrays, we used traditional strategies such as confirmation of gene changes with RT-PCR. It is generally accepted that RT-PCR is more reliable than microarray analysis when it comes to individual genes.[25] Although the change in expression detected by RT-PCR is not necessarily the same as that determined by microarray analysis, such differences are attributed to the different methodology used, as long as the direction of change is the same. However, RT-PCR analysis can be performed on only a limited number of genes. We elected the genes to confirm by RT-PCR on the basis that they participate in different genetic networks. Our purpose was to confirm at least one of the genes with changing expression in each network, thus adding credibility that the network was involved in the pathology.

Changes in gene expression do not by themselves affect cellular physiology unless they are followed by changes in protein production. Confirmation of the changes in protein amounts for every gene differentially expressed is beyond the scope of this experimental work. The very limited amount of protein that can be extracted from small regions of a single retina makes this task very challenging. However, we did confirm that the protein expression of at least one of the downregulated and one of the upregulated genes changed in damaged versus spared areas of the glaucomatous mouse retina. These two proteins with expression changes that we confirmed are Osbpl9 (ORP9) and SNBT2 (syntrophin 2), respectively.

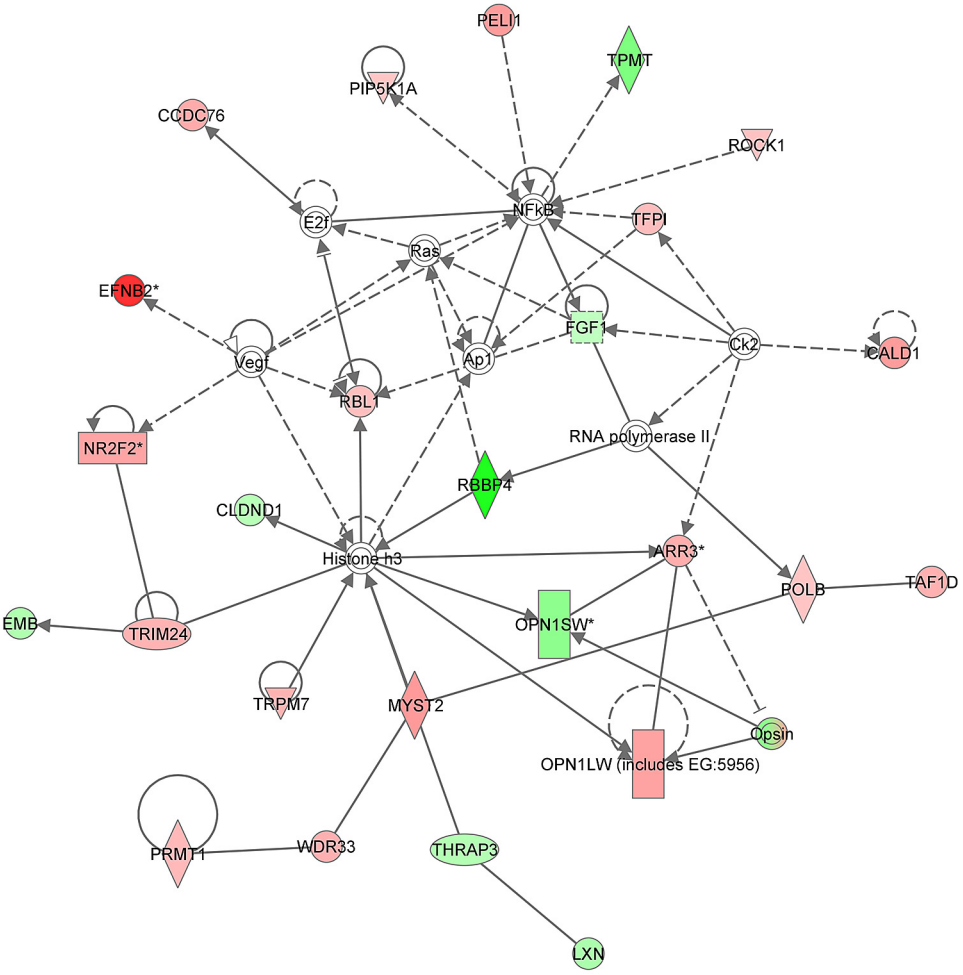

FIGURE 2. Functional network of genes with differential expression between damaged and spared retinal areas in DBA/2 mice. *Green shades*: downregulated genes; *red shades*: upregulated genes. This is the network most heavily populated by differentially expressed genes. A total of 22 such networks were identified. *Ap1*, activator protein 1; *Arr3*, retinal arrestin 3; *CALD1*, caldesmon 1; *CCDC76*, coiled-coil domain containing 76; *Ck2*, casein kinase II, alpha prime polypeptide; *CLDND1*, claudin domain containing 1; *E2f*, E2F transcription factor; *EFNB2*, ephrin B2; *EMB*, embigin; *FGF1*, fibroblast growth factor 1; *LXN*, latexin; *MYST2*, MYST histone acetyltransferase 2; *NFKB*, nuclear factor of kappa light polypeptide gene enhancer in B-cells; *NR2F2*, nuclear receptor subfamily 2, group F, member 2; *OPN1SW*, opsin 1 (cone pigments), short-wave-sensitive (color blindness, tritan); *PELI1*, pellino 1; *PIP5K1A*, phosphatidylinositol-4-phosphate 5-kinase, type 1 alpha; *POLB*, beta polymerase (DNA directed); *PRMT1*, protein arginine N-methyltransferase 1; *Ras*, resistance to audiogenic seizures; *RBBP4*, retinoblastoma binding protein 4; *RBL1*, retinoblastoma-like 1 (p107); *TAF1D*, TATA box binding protein (Tbp)-associated factor RNA polymerase I D; *TFPI*, tissue factor pathway inhibitor; *THRAP3*, thyroid hormone receptor associated protein 3; *TPMT*, thiopurine methyltransferase; *TRIM24*, tripartite motif-containing 24; *TRPM7*, transient receptor potential cation channel subfamily M member 7; *Vegf*, vascular endothelial growth factor; and *WDR33*, WD repeat domain 33.

Osbpl9/ORP9 belongs to a large family of oxysterol-binding (OSBP) and OSBP-related proteins (ORP) that has been conserved between yeast and humans.[26,27] Oxysterols regulate cholesterol biosynthesis, uptake, and efflux,[28] but also other biological functions through the liver nuclear receptors (LXRs)[29] that are present in many tissues, including the retina.[30] ORPs have a pleckstrin homology (PH) domain[31] that mediates interaction with phosphatidyl-inositol 4 phosphate (PI-4-P) and is crucial for targeting the proteins to the Golgi complex.[32] They also carry an FFAT consensus sequence that binds VAMP-associated proteins targeting the ORPs to the endoplasmic reticulum.[33] OSBPL9 (or ORP9, as otherwise known) also has a Golgi targeting sequence in its amino terminal end and has been proposed to be a Golgi regulating, cholesterol transfer protein.[34] Although the exact function of each of the ORPs is yet unclear, studies have suggested that they participate in lipid metabolism and act as sensors and transporters of cholesterol and sphingolipids[31,32,35] and that they participate in cell signaling by regulating the activity of the ERK/MAPK pathways.[36] OSBPL9/ORP9 contains a PKC-β phosphorylation site,[37] allowing it to negatively regulate the PDK-2 site at Akt, which is known to control cell survival, cell cycle progression, and glucose metabolism.[37] Thus, upregulation of ORP9 in areas of the retina with extensive damage indicated by RGC loss may result from local signals that involve rapidly diffusible lipids and affect the ER and Golgi apparatus. After all, many of the proteins that are associated with glaucoma in humans appear to have a function in ER/Golgi/endosomal trafficking.[38,39]

Syntrophins are a family of widely distributed intracellular peripheral membrane proteins with two tandem PH domains followed by a syntrophin-unique C terminus domain. They also have a single PDZ domain[40] through which they most likely bind to sodium channels.[41,42] They also have the ability to bind to sodium and potassium channels through other domains or intermediate proteins[42] and may regulate the proper localization and physiological function of these channels. In addition, syntrophins are known to bind nitric oxide synthase (nNOS), helping to target the enzyme to the sarcolemma.[43–45] β2-Syntrophin has been found in the neuromuscular junction[46] and has been shown to colocalize and interact with a family of microtubule-associated protein kinases.[47] The function of β-syntrophin in the retina is currently unknown, but other members of the syntrophin family have been implicated in regulation of subcellular localization of aquaporin 4[48] and potassium channels in Müller cells.[49–51] This localization raises the possibility that altered water and electrolyte subcellular distribution may modify the function of Müller cell endfeet sufficiently to produce an environment that is detrimental for RGC survival.[52] Alternatively, it could be the result of RGC loss.

Investigators studying gene expression and drug development have recently come to the realization that for most genetically complex disorders, it is unlikely that altering the expression or activity of a single gene could be used as a treatment.[53] Instead, genes can be thought of as parts of networks that are affected in pathologic conditions. It is thus important to look at the broader context in which a particular set of genes operates and try to deduce information on the

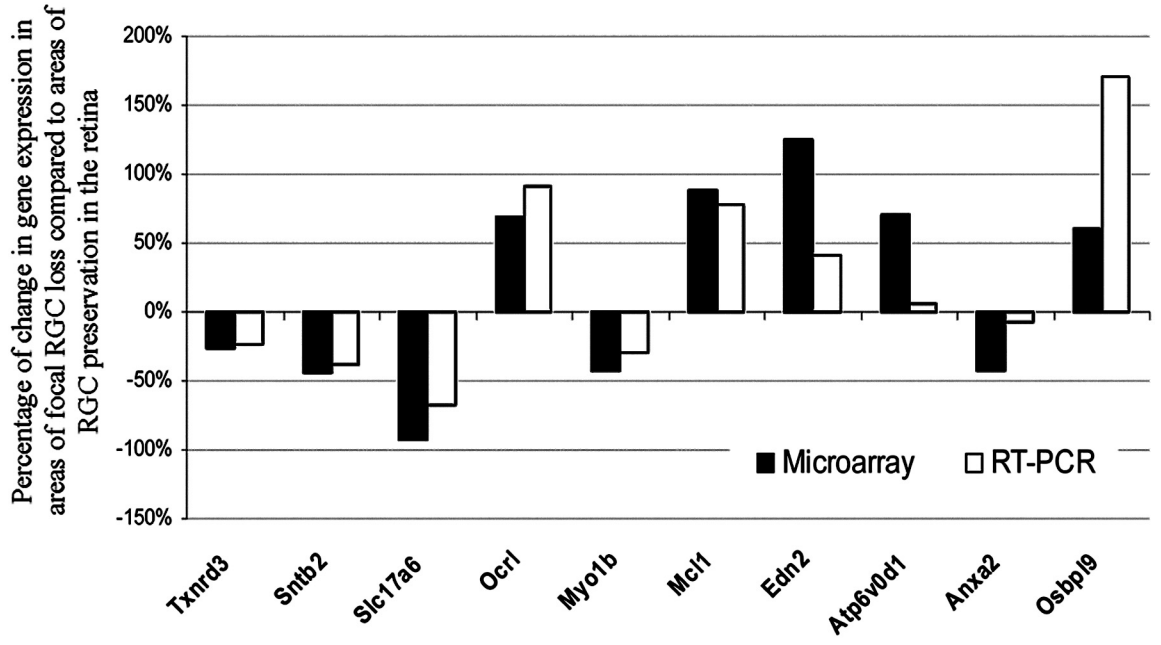

FIGURE 3. Percentage of change of gene expression between damaged and spared retinal areas in DBA/2 mice by microarray analysis and confirmed by RT-PCR. Note that the difference determined with the two methods was not identical, but changes were detected in the same direction by both methods. *Txnrd3*, thioredoxin reductase 3; *Sntb2*, β2-syntrophin; *Slc17a6*, solute carrier family 17 (sodium-dependent inorganic phosphate cotransporter), member 6; *Ocrl*, oculocerebrorenal syndrome of Lowe; *Myo1b*, myosin IB; *Mcl1*, myeloid cell leukemia sequence 1; *Edn2*, endothelin 2; *Atp6v0d1*, ATPase H+ transporting V0, subunit D, isoform 1; *Anxa2*, annexin 2; *Osbpl9*, oxysterol binding protein-like 9.

pathophysiology of various conditions. Network analysis places the genes of interest on diagrams that describe well-known relationship networks that have been reported in the literature. Similarly, canonical pathways analysis also provides information as to how likely it is that a certain number of genes will appear in the same network. By using network and canonical pathways analysis, we identified several important gene networks that appear to be at an increased operational level in glaucoma.

One of the networks identified is presented in Figure 2. Although this is not the only network identified, we present it as example of a network that can be used for developing targeted therapies. In this particular network, ~75% of the genes were identified as having different expression between damaged and spared retinal areas. Although this was the network with the highest score identified, the percentage of genes affected in each of the other networks identified was at least 23%. Eighty percent of the networks identified had at least 40% of their genes differentially expressed. It is important to understand that, given the limitations of microarray experiments, not all molecular components on a network will show altered expression. For example, expression of regulatory molecules is unlikely to change enough to allow detection. What is significant is that a sufficient number of molecules within a network change at the same time. This discovery provides convincing evidence that the activity of the network is altered.

One of the most affected pathways identified was the phototransduction pathway. Despite the lack of gross morphologic changes in the photoreceptors in the DBA/2 mouse, previous publications have shown changes in gene expression and morphology of the photoreceptors in primate glaucomatous retinas.[54,55]

As mentioned previously, results of network analysis (as well as the gene clusters identified with DAVID analysis) are somewhat arbitrary and depend on our existing knowledge of relationships between various genes. As our understanding of the cell physiology and interactions increases, membership in

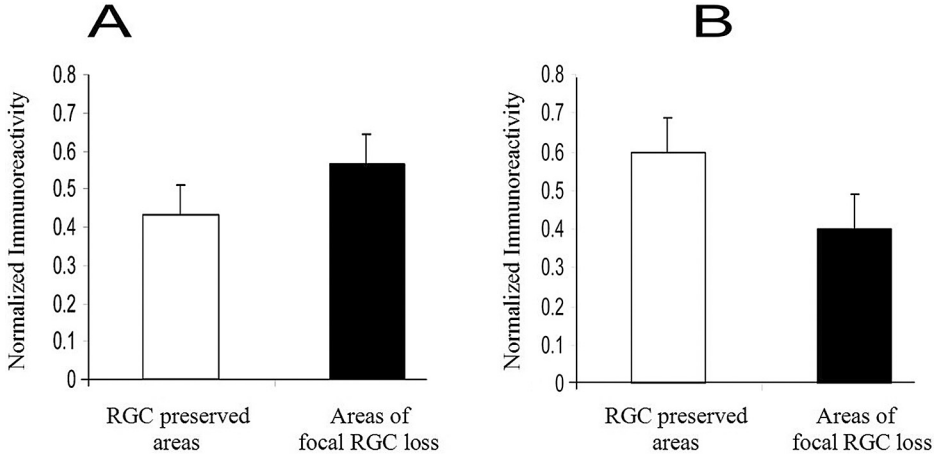

FIGURE 4. Osbpl-9 and β2-syntrophin immunoreactivity in damaged and spared retinal areas. Staining was normalized to the amount of β-actin, to account for potential differences in the amount of protein loaded in each lane. Osbpl-9 immunoreactivity (**A**) was upregulated in areas of focal ganglion cell loss, whereas β2-syntrophin (**B**) immunoreactivity was downregulated. Error bars represent SEM from 2 different Western blot membranes. Each sample contains protein from a pool of four retinas.

these networks is bound to change somewhat. In addition, as also mentioned, these networks will become more and more overlapping. What is important is that they provide a framework for confirming that individual genes are involved in a process and exploring how related genes are also affected.

We initiated this work by reasoning that, by studying the gene expression differences between spared and damaged areas in the same retinas in paired fashion, we would be able to determine several things.

1. Some genes may be responsible for or contribute to RGC loss. Such genes may be up- (or down-) regulated before RGC loss in the retina (not necessarily in the RGCs) and their expression could return to baseline levels after RGC loss.
2. There are genes expression that undergoes sustained change in reaction to RGC loss. Such genes expressed in other (non-RGC) retinal cells could be up- or downregulated as a result of changes in the retinal environment after the death of RGCs.
3. There are genes that are RGC specific: These genes would be severely downregulated in areas of the retina with severe RGC loss.

One has of course to keep in mind that there may also be "causative" genes, as in no. 1, with expression that does not return to baseline levels after RGC loss. Such genes would not necessarily be detected by comparing damaged with spared retinal areas, as their expression would also be expected to change in healthy retinal areas before RGC loss. For genes that are expressed at a very low level, it would be difficult to show differences in expression using the whole retina. It is reasonable to assume that some of the gene networks that lead to RGC loss are operational in the spared areas (as these would also progress to RGC loss subsequently), whereas networks of genes that are turned on or off as a result of RGC loss would be operational in the damaged areas. On the other hand, the major advantage of analyzing gene expression in the retina (rather than only RGC gene expression) does not presuppose that the pathogenic mechanisms of glaucoma involve only one cell type. Evidence from our laboratory[56] as well as from other investigators[57,58] indicates that the sequence of events leading to RGC death may originate or depend on other cells in the retina. Focusing on gene and protein expression only in RGCs (using for example cell cultures) may result in missing key genes involved in the development or progression of glaucoma.

RGC-specific genes are of course expected to be completely downregulated in areas of extensive RGC loss. However, one has to keep in mind that RGCs account for $<1\%$ of the retinal cells, and thus even complete focal RGC loss would not result in detectable changes in genes expressed in RGCs, unless they are uniquely RGC specific. Even then, because of the intensity cutoffs used, some of these genes may not be detected as changing. Indeed, some of the RGC-specific genes were detected to be significantly downregulated in damaged areas (see for example the *Opa1* gene) whereas others (e.g., *Brn-3* or *Thy-1*) were not. An alternative explanation may be that the expression of some of the RGC-specific genes may be downregulated before the cells themselves are lost.[59,60]

We used the pearl strain as an additional nonpathologic control for these experiments with the idea that gene expression in the retina of this strain would be similar to that in preserved areas with minimal RGC loss in DBA/2 mice. Pearl mice carry both the *Tyrp1* and *Gpnmb* mutations that are responsible for RGC loss in the DBA/2 strain, but also carry the pearl coat color mutation. This actually consists of a deletion of approximately 100 bp of the *Ap3b1* gene, rendering it nonfunctional.[61,62] As a consequence, melanin processing is completely disrupted, and thus the animals have a characteristically white coat. More important, they do not have high IOP or undergo RGC loss,[5] at least up to the 15th month of age. Because they are on a DBA/2 background, they were an almost ideal control for the microarray experiments described herein. Although minor differences are bound to exist between animals that are maintained in separate colonies and it is possible that the introduction of the *Ap3b1* mutation leads to significant gene expression profile changes, at the time this work was performed, pearl mice were the genetically closest control animals we could find. We decided against the alternative strategy of using younger DBA/2 prepathologic mice as the control because of the potential effect that age-related changes in gene expression may have. Based on the PCA results, it is evident that spared areas with RGC preservation within the DBA/2 retinas are far from normal and have a gene expression profile very different from that in the normal retina of pearl mice. Roughly 60% of the genes with different expression between damaged and spared retinal areas of the DBA/2 mice have levels of expression in the pearl retina that conform with our assumption (i.e., levels in pearl retinas are similar to those in damaged DBA/2 areas or follow a graded difference—from pearl retina, to damaged D2 areas, to spared D2 areas). The levels of expression of the other 40% were more similar between pearl retinas and damaged areas in DBA/2 retinas, suggesting a return to more normal retinal gene expression (and by extension retinal physiology) once RGCs are lost.

One of the major limitations of this study is related to one of its major strengths. Because we looked at gene expression in the whole retina, the experiments described herein could not distinguish between gene expression within specific retinal cell types. Methods of localization of gene expression do exist at both the mRNA and protein levels but unfortunately are currently semiquantitative at best when large areas of the retina need to be sampled. We are currently trying to determine where within the retina some of these genes are differentially expressed using ISH and immunohistochemistry. Such localization will undoubtedly provide a clearer picture as to what are the underlying pathophysiologic mechanisms for RGC loss in glaucoma.

References

1. John SW, Smith RS, Savinova OV, et al. Essential iris atrophy, pigment dispersion, and glaucoma in DBA/2J mice. *Invest Ophthalmol Vis Sci.* 1998;39:951–962.
2. Aihara M, Lindsey JD, Weinreb RN. Experimental mouse ocular hypertension: establishment of the model. *Invest Ophthalmol Vis Sci.* 2003;44:4314–4320.
3. Ruiz-Ederra J, Verkman AS. Mouse model of sustained elevation in intraocular pressure produced by episcleral vein occlusion. *Exp Eye Res.* 2006;82:879–884.
4. Sheldon WG, Warbritton AR, Bucci TJ, Turturro, A. Glaucoma in food-restricted and ad libitum-fed DBA/2NNia mice. *Lab Anim Sci.* 1995;45:508–518.
5. Anderson MG, Smith RS, Hawes NL, et al. Mutations in genes encoding melanosomal proteins cause pigmentary glaucoma in DBA/2J mice. *Nat Genet.* 2002;30:81–85.
6. Danias J, Lee KC, Zamora MF, et al. Quantitative analysis of retinal ganglion cell (RGC) loss in aging DBA/2NNia glaucomatous mice: comparison with RGC loss in aging C57/BL6 mice. *Invest Ophthalmol Vis Sci.* 2003;44:5151–5162.
7. Schlamp CL, Li Y, Dietz JA, Janssen KT, Nickells, RW. Progressive ganglion cell loss and optic nerve degeneration in DBA/2J mice is variable and asymmetric. *BMC Neurosci.* 2006;7:66.
8. Jakobs TC, Libby RT, Ben Y, John SW, Masland RH. Retinal ganglion cell degeneration is topological but not cell type specific in DBA/2J mice. *J Cell Biol.* 2005;171:313–325.

9. Hubbell E, Liu WM, Mei R. Robust estimators for expression analysis. *Bioinformatics.* 2002;18:1585–1592.
10. Wu Z, Irizarry RA. Stochastic models inspired by hybridization theory for short oligonucleotide arrays. *J Comput Biol.* 2005;12:882–893.
11. Gentleman RC, Carey VJ, Bates DM, et al. Bioconductor: open software development for computational biology and bioinformatics. *Genome Biol.* 2004;5:R80.
12. Anderson MG, Libby RT, Gould DB, Smith RS, John SW. High-dose radiation with bone marrow transfer prevents neurodegeneration in an inherited glaucoma. *Proc Natl Acad Sci U S A.* 2005;102:4566–4571.
13. Filippopoulos T, Danias J, Chen B, Podos SM, Mittag TW. Topographic and morphologic analyses of retinal ganglion cell loss in old DBA/2NNia mice. *Invest Ophthalmol Vis Sci.* 2006;47:1968–1974.
14. Kurian KM, Watson CJ, Wyllie AH. DNA chip technology. *J Pathol.* 1999;187:267–271.
15. Bednar M. DNA microarray technology and application. *Med Sci Monit.* 2000;6:796–800.
16. Hofman P. DNA microarrays. *Nephron Physiol.* 2005;99:85–89.
17. Chen JJ, Hsueh HM, Delongchamp RR, Lin CJ, Tsai, CA. Reproducibility of microarray data: a further analysis of microarray quality control (MAQC) data. *BMC Bioinformatics.* 2007;8:412.
18. Hernandez MR, Agapova OA, Yang P, Salvador-Silva M, Ricard CS, Aoi S. Differential gene expression in astrocytes from human normal and glaucomatous optic nerve head analyzed by cDNA microarray. *Glia.* 2002;38:45–64.
19. Ishibashi T, Takagi Y, Mori K, et al. cDNA microarray analysis of gene expression changes induced by dexamethasone in cultured human trabecular meshwork cells. *Invest Ophthalmol Vis Sci.* 2002;43:3691–3697.
20. Yoshimura N. Retinal neuronal cell death: molecular mechanism and neuroprotection (in Japanese). *Nippon Ganka Gakkai Zasshi.* 2001;105:884–902.
21. Piri N, Kwong JM, Song M, Elashoff D, Caprioli J. Gene expression changes in the retina following optic nerve transection. *Mol Vis.* 2006;12:1660–1673.
22. Steele MR, Inman DM, Calkins DJ, Horner PJ, Vetter ML. Microarray analysis of retinal gene expression in the DBA/2J model of glaucoma. *Invest Ophthalmol Vis Sci.* 2006;47:977–985.
23. Miyahara T, Kikuchi T, Akimoto M, Kurokawa T, Shibuki H, Yoshimura N. Gene microarray analysis of experimental glaucomatous retina from cynomolgus monkey. *Invest Ophthalmol Vis Sci.* 2003;44:4347–4356.
24. Miao H, Chen L, Riordan SM, et al. Gene expression and functional studies of the optic nerve head astrocyte transcriptome from normal African Americans and Caucasian Americans donors. *PLoS ONE.* 2008;3:e2847.
25. Etienne W, Meyer MH, Peppers J, Meyer RA Jr. Comparison of mRNA gene expression by RT-PCR and DNA microarray. *BioTechniques.* 2004;36:618–620,622,624–626.
26. Jiang B, Brown JL, Sheraton J, Fortin N, Bussey H. A new family of yeast genes implicated in ergosterol synthesis is related to the human oxysterol binding protein. *Yeast.* 1994;10:341–353.
27. Lehto M, Laitinen S, Chinetti G, et al The OSBP-related protein family in humans. *J Lipid Res.* 2001;42:1203–1213.
28. Venkateswaran A, Laffitte BA, Joseph SB, et al. Control of cellular cholesterol efflux by the nuclear oxysterol receptor LXR alpha. *Proc Natl Acad Sci U S A.* 2000;97:12097–12102.
29. Whitney KD, Watson MA, Goodwin B, et al. Liver X receptor (LXR) regulation of the LXRalpha gene in human macrophages. *J Biol Chem.* 2001;276:43509–43515.
30. Moreira EF, Larrayoz IM, Lee JW, Rodriguez IR. 7-Ketocholesterol is present in lipid deposits in the primate retina: potential implication in the induction of VEGF and CNV formation. *Invest Ophthalmol Vis Sci.* 2009;50:523–532.
31. Johansson M, Bocher V, Lehto M, et al The two variants of oxysterol binding protein-related protein-1 display different tissue expression patterns, have different intracellular localization, and are functionally distinct. *Mol Biol Cell.* 2003:14:903–915.
32. Balla A, Tuymetova G, Tsiomenko A, Varnai P, Balla T. A plasma membrane pool of phosphatidylinositol 4-phosphate is generated by phosphatidylinositol 4-kinase type-III alpha: studies with the PH domains of the oxysterol binding protein and FAPP1. *Mol Biol Cell.* 200:16:1282–1295.
33. Wyles JP, Ridgway ND. VAMP-associated protein-A regulates partitioning of oxysterol-binding protein-related protein-9 between the endoplasmic reticulum and Golgi apparatus. *Exp Cell Res.* 2004;297:533–547.
34. Ngo M, Ridgway ND. Oxysterol binding protein (OSBP)-related Protein 9 (ORP9) is a cholesterol transfer protein that regulates Golgi structure and function. *Mol Biol Cell.* 2009;20:1388–1399.
35. Im YJ, Raychaudhuri S, Prinz WA, Hurley JH. Structural mechanism for sterol sensing and transport by OSBP-related proteins. *Nature.* 2005;437:154–158.
36. Wang PY, Weng J, Anderson RG. OSBP is a cholesterol-regulated scaffolding protein in control of ERK 1/2 activation. *Science.* 2005;307:1472–1476.
37. Lessmann E, Ngo M, Leitges M, Minguet S, Ridgway ND, Huber M. Oxysterol-binding protein-related protein (ORP) 9 is a PDK-2 substrate and regulates Akt phosphorylation. *Cell Signal.* 2007;19:384–392.
38. Park BC, Shen X, Samaraweera M, Yue BY. Studies of optineurin, a glaucoma gene: Golgi fragmentation and cell death from overexpression of wild-type and mutant optineurin in two ocular cell types. *Am J Pathol.* 2006;169:1976–1989.
39. Malyukova I, Lee HS, Fariss RN, Tomarev SI. Mutated mouse and human myocilins have similar properties and do not block general secretory pathway. *Invest Ophthalmol Vis Sci.* 2006;47:206–212.
40. Ahn AH, Kunkel LM. Syntrophin binds to an alternatively spliced exon of dystrophin. *J Cell Biol.* 1995;128:363–371.
41. Schultz J, Hoffmuller U, Krause G, et al. Specific interactions between the syntrophin PDZ domain and voltage-gated sodium channels. *Nat Struct Biol.* 1998;5:19–24.
42. Gee SH, Madhavan R, Levinson SR, Caldwell JH, Sealock R, Froehner SC. Interaction of muscle and brain sodium channels with multiple members of the syntrophin family of dystrophin-associated proteins. *J Neurosci.* 1998;18:128–137.
43. Brenman JE, Chao DS, Gee SH, et al. Interaction of nitric oxide synthase with the postsynaptic density protein PSD-95 and alpha1-syntrophin mediated by PDZ domains. *Cell.* 1996;84:757–767.
44. Chamberlain JS, Corrado K, Rafael JA, Cox GA, Hauser M, Lumeng C. Interactions between dystrophin and the sarcolemma membrane. *Soc Gen Physiol Ser.* 1997;52:19–29.
45. Miyagoe-Suzuki Y, Takeda, S.I. Association of neuronal nitric oxide synthase (nNOS) with alpha1-syntrophin at the sarcolemma. *Microsc Res Technol.* 2001;55:164–170.
46. Peters MF, Kramarcy NR, Sealock R, Froehner SC. beta 2-Syntrophin: localization at the neuromuscular junction in skeletal muscle. *Neuroreport.* 1994;5:1577–1580.
47. Lumeng C, Phelps S, Crawford GE, Walden PD, Barald K, Chamberlain JS. Interactions between beta 2-syntrophin and a family of microtubule-associated serine/threonine kinases. *Nat Neurosci.* 1999;2:611–617.
48. Neely JD, Amiry-Moghaddam M, Ottersen OP, Froehner SC, Agre P, Adams ME. Syntrophin-dependent expression and localization of Aquaporin-4 water channel protein. *Proc Natl Acad Sci U S A.* 2001;98:14108–14113.
49. Noel G, Belda M, Guadagno E, Micoud J, Klocker N, Moukhles H. Dystroglycan and Kir4.1 coclustering in retinal Muller glia is regulated by laminin-1 and requires the PDZ-ligand domain of Kir4.1. *J Neurochem.* 2005;94:691–702.
50. Connors NC, Kofuji P. Potassium channel Kir4.1 macromolecular complex in retinal glial cells. *Glia.* 2006;53:124–131.
51. Puwarawuttipanit W, Bragg AD, Frydenlund DS, et al. Differential effect of alpha-syntrophin knockout on aquaporin-4 and Kir4.1 expression in retinal macroglial cells in mice. *Neuroscience.* 2006;137:165–175.
52. Rurak J, Noel G, Lui L, Joshi B, Moukhles H. Distribution of potassium ion and water permeable channels at perivascular glia in brain and retina of the Large(myd) mouse. *J Neurochem.* 2007;103:1940–1953.
53. Breakthrough of the year: the runners-up. *Science.* 2008;322:1768.
54. Nork TM, Ver Hoeve JN, Poulsen GL, et al. Swelling and loss of photoreceptors in chronic human and experimental glaucomas. *Arch Ophthalmol.* 2000;118:235–245.

55. Pelzel HR, Schlamp CL, Poulsen GL, Ver Hoeve JA, Nork TM, Nickells RW. Decrease of cone opsin mRNA in experimental ocular hypertension. *Mol Vis.* 2006;12:1272–1282.
56. Stasi K, Nagel D, Yang X, et al. Complement component 1Q (C1Q) upregulation in retina of murine, primate, and human glaucomatous eyes. *Invest Ophthalmol Vis Sci.* 2006;47:1024–1029.
57. Wax MB, Tezel G, Yang J, et al. Induced autoimmunity to heat shock proteins elicits glaucomatous loss of retinal ganglion cell neurons via activated T-cell-derived fas-ligand. *J Neurosci.* 2008; 28:12085–12096.
58. Bosco A, Inman DM, Steele MR, et al. Reduced retina microglial activation and improved optic nerve integrity with minocycline treatment in the DBA/2J mouse model of glaucoma. *Invest Ophthalmol Vis Sci.* 2008;49:1437–1446.
59. Surgucheva I, McMahan B, Ahmed F, Tomarev S, Wax MB, Surguchov A. Synucleins in glaucoma: implication of gamma-synuclein in glaucomatous alterations in the optic nerve. *J Neurosci Res.* 2002;68:97–106.
60. Huang W, Fileta J, Guo Y, Grosskreutz, CL. Downregulation of Thy1 in retinal ganglion cells in experimental glaucoma. *Curr Eye Res.* 2006;31:265–271.
61. Feng L, Rigatti BW, Novak EK, Gorin MB, Swank RT. Genomic structure of the mouse Ap3b1 gene in normal and pearl mice. *Genomics.* 2000;69:370–379.
62. Feng L, Seymour AB, Jiang S, et al. The beta3A subunit gene (Ap3b1) of the AP-3 adaptor complex is altered in the mouse hypopigmentation mutant pearl, a model for Hermansky-Pudlak syndrome and night blindness. *Hum Mol Genet.* 1999;8:323–330.